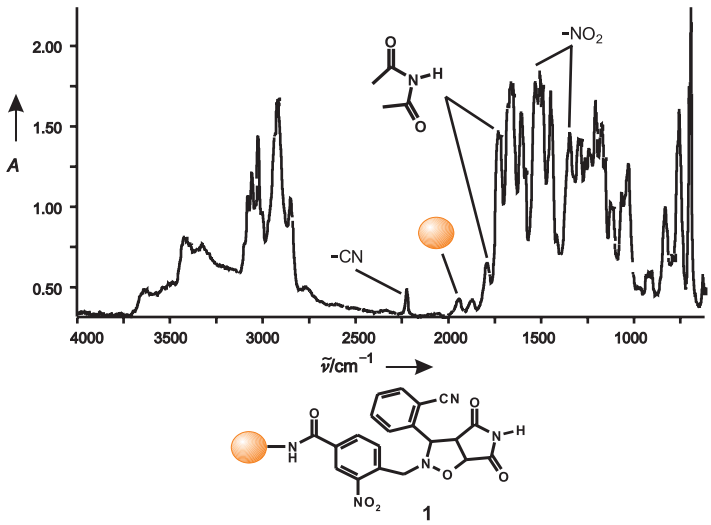

Figure 6. FT-IR spectrum of an individual resin bead on which **1** is immobilized.

method can thus provide a valuable contribution to the development of miniaturized syntheses on individual resin beads. The combination of IR mapping with MS and HPLC-MS analysis means that tagging concepts can be abandonned; technical procedures of automatic sorting of resin beads could even be developed.

Experimental Section

The FT-IR mapping was carried out with a Bruker IRScope II instrument. The resin beads modified according to Scheme 1 were embedded in a KBr window under a slight pressure. An area of 3×3 mm^2 was mapped with an IR microscope. With a step width of 50 μm 60 data points were measured in the x as well as the y direction, so that a total of 3600 IR spectra were registered for the IR mapping. For a resolution of 4 cm^{-1} and a summation of 4 scans per data point, the measurement time was 5 h.

Received: May 13, 1998 [Z11849IE]
German version: *Angew. Chem.* **1998**, *110*, 3506 – 3509

Keywords: combinatorial chemistry · IR spectroscopy · microscopy · solid-phase syntheses

[1] F. Balkenhohl, C. von dem Bussche-Hünnefeld, A. Lansky, C. Zechel, *Angew. Chem.* **1996**, *108*, 2436 – 2488; *Angew. Chem. Int. Ed. Engl.* **1996**, *35*, 2289 – 2337.
[2] J. S. Früchtel, G. Jung, *Angew. Chem.* **1996**, *108*, 19 – 46; *Angew. Chem. Int. Ed. Engl.* **1996**, *35*, 17 – 42.
[3] E. M. Gordon, M. A. Gallop, D. V. Patel, *Acc. Chem. Res.* **1996,** *29*, 144 – 154.
[4] *Combinatorial Peptide and Non-peptide Libraries* (Ed.: G. Jung), VCH, Weinheim, **1996**.
[5] L. A. Thompson, J. A. Ellmann, *Chem. Rev.* **1996**, *96*, 555 – 600.
[6] P. H. H. Hermkens, H. C. J. Ottenheijm, D. C. Rees, *Tetrahedron* **1997**, *53*, 5643 – 5678.
[7] M. Pursch, G. Schlotterbeck, L.-H. Tseng, K. Albert, W. Rapp, *Angew. Chem.* **1996**, *108*, 3043 – 3036; *Angew. Chem. Int. Ed. Engl.* **1996**, *35*, 2867 – 2869.
[8] S. K. Sarkar, R. Garigipati, J. L. Adams, P. A. Keifer, *J. Am. Chem. Soc.* **1996**, *118*, 2305 – 2306.
[9] a) B. Yan, G. Kumaravel, H. Anjaria, A. Wu, R. C. Petter, C. F. Jewell, Jr., J. R. Wareing, *J. Org. Chem* **1995**, *60*, 5736 – 5738; b) B. Yan, J. B. Fell, G. Kumaravel, *J. Org. Chem.* **1996**, *61*, 7467 – 7472.
[10] B. Yan, G. Kumaravel, *Tetrahedron* **1996**, *52*, 843.
[11] a) K. Russell, D. C. Cole, F. M. McLaren, D. E. Pivonka, *J. Am. Chem. Soc.* **1996**, *118*, 7941 – 7945; b) D. E. Pivonka, K. Russell, T. Giero, *Appl. Spectr.* **1996**, *50*, 1471.
[12] W. J. Haap, D. Kaiser, T. B. Walk, G. Jung, *Tetrahedron* **1998**, *54*, 3705 – 3724.
[13] A. Furka, F. Sebestyen, M. Asgedom, G. Dibo, *Int. J. Pept. Protein Res.* **1991**, *37*, 487 – 493.

Ba_3Ge_4: Polymerization of Zintl Anions in the Solid and Bond Stretching Isomerism**

Fabio Zürcher and Reinhard Nesper*

In memory of Jean Rouxel

In the fast-growing family of Zintl phases, an ever-increasing number of completely new bonding patterns of main group element clusters, Zintl anions, are being discovered. These oligo anions or polyanions often carry relatively high formal charges, which can be determined in accordance with the Zintl – Klemm concept.[1] In the solid, stabilization is achieved through a large number of surrounding cations. The transfer to solution has only been successful in a few cases until now, most of which were Zintl anions with low formal charges.[2] It has not yet proved possible to directly dissolve the smaller, highly charged oligomeric anions of Group 14 elements such as E_4^{4-},[3] E_4^{6-},[4] E_8^{16-},[5–7] E_{12}^{21-}[6–8] from the Zintl phase into solution. Apart from E_4 in the form of a tetrahedron[9] or a butterfly anion, none of these has even been synthesized as a molecular compound.

We investigated the different effects of cations on the Zintl anions in a series of experiments and were able to detect a strong relationship between the polyanion E_n^{m-} formed and the type of cation used. Small, polarizing cations, in particular Mg^{2+} and complex cations such as M_6X^{10+} (M = Ca, Sr, Ba; X = O) thus favor the formation of highly charged end groups or isolated E^{4-} ions. In contrast, large mononuclear cations preferentially stabilize E–E bonds, whereby the E atoms are less highly charged.[7] According to the Zintl – Klemm concept, semiconductor structures can only be formed in which the polyanions E_n^{m-} follow the $8-N$ rule or the cluster counting rules. There are often several structural solutions for a given composition and valence electron number, however, and then the factors mentioned above also play a part in determining the form of the Zintl anion formed. The influence of cation size in determining the structure of the polyanion type for a given electron number has been little investigated

[*] Prof. Dr. R. Nesper, Dr. F. Zürcher
Laboratorium für Anorganische Chemie, ETH Zurich
Universitätstrasse 6, CH-8092 Zurich (Switzerland)
Fax: +(41) 1-632-1149
E-mail: nesper@inorg.chem.ethz.ch
[**] This work was supported by the Schweizerischen Nationalfonds zur Förderung der wissenschaftlichen Forschung (project no. 20-43228.95).

  1433-7851/98/3723-3314 $ 17.50+.50/0

until now. We have now found a borderline case with Ba_3Ge_4, which shows very clearly just this effect.

Of the binary Ba/Ge phases,[10] only the compounds Ba_2Ge,[11] BaGe,[12] and $BaGe_2$[13] have been characterized to date. Despite several indications for a phase with the composition Ba_3Ge_4,[14] this has not been described in more detail as yet. In contradiction to the published phase diagram,[10] we have now obtained Ba_3Ge_4 from a stoichiometric reaction of the elements between 1120 and 1360 K.[15]

There are two modifications of Ba_3Ge_4:[16] Above 630 K the β-Ba_3Ge_4 phase, isotypic with Ba_3Si_4, is stable, whereas the room-temperature phase α-Ba_3Ge_4 crystallizes in a new structural type.[16, 17] This is admittedly not isotypic with Ba_3Si_4, but it is related to it. According to the observed abrupt changes in volume and enthalpy the phase transition from the α to the β form cannot be second order and thus must be discontinuous. However, by careful warming of single crystals of α-Ba_3Ge_4 on the diffractometer these were converted into single crystals of β-Ba_3Ge_4, which were then measured. Slow cooling led to the reformation of the α form, but the single crystals were completely destroyed. Whereas Ba_3Si_4 contains exclusively isolated Si_4^{6-} butterfly anions (Figure 1a), in addition to the monomer the chainlike cross-linked polymer made up of butterfly anions of Ge_4^{6-} occurs in α-Ba_3Ge_4 (Figure 1b). We attribute this to the size of the Ba^{2+} ions being insufficient to separate the anions far enough from one another and thus stabilize the monomers. The anions are able to approach one another, leading to the polymerization of half of these groups with a simultaneous and considerable anisotropic reduction in volume of the unit cell. An orthorhombic distortion of the unit cell occurs, in which only the Zintl anions in the crystallographic a axis are linked

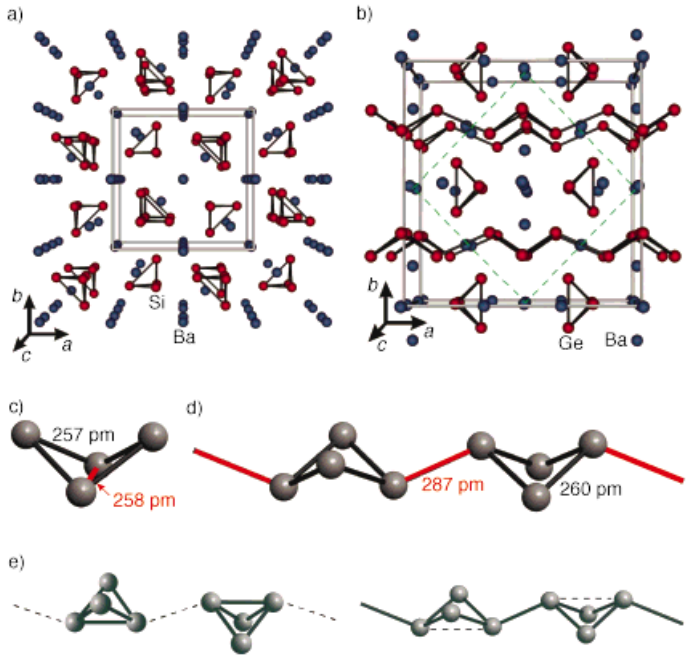

Figure 1. Structures of a) Ba_3Si_4 and b) α-Ba_3Ge_4. The position of the unit cell in (a) is indicated by green lines in (b). c) Isolated butterfly unit. d) Polymeric chain of butterfly anions. e) Geometric relationship between the arrangement of monomeric and polymeric butterfly anions.

(Figure 1b). The accompanying shortening in length is about 3%, whereas the other two axes remain almost unchanged.

The Zintl–Klemm concept is fulfilled by both modifications in different ways: $(Ba^{2+})_6[Ge_4^{6-}]$ $^1_\infty[Ge_4^{6-}]$ satisfies the $8-N$ rule just as does the $(Ba^{2+})_3[Ge_4^{6-}]$ modification made up entirely of monomers. The isolated butterfly anions E_4^{6-} contain two-valent and three-valent species $(2b)E^{2-}$ and $(3b)E^-$ with two or one free electron pair(s), respectively. In the polymer, the intermolecular linkage ($d(Ge{-}Ge)_{inter}$ = 287.4(2) pm) replaces the central intramolecular bond in the butterfly anion ($d(Ge{-}Ge)_{intra}$ = 327.4(3) pm; Figures 1c and 1d). Thus, neither the number of bonds, nor the charges are changed; the two-valent and three-valent germanium species $(2b)Ge^{2-}$ and $(3b)Ge^-$ are not swapped during the polymerization (Figures 1e).

According to experimental and theoretical studies on the neutral bicyclo[1.1.0] systems Si_4R_6 and $E_2C_2R_6$, this intramolecular bond possesses unusual properties even in the monomer. From structural investigations, both species with normal single bond lengths (d(Si–Si) = 237 pm) and those with very long central bonds (d(C–C = 178 pm) are known.[18–20] Results are available from quantum-mechanical calculations on Si_4H_6. Although these are of varying quality, they all confirm a double minimum potential with d_1(Si–Si) = 234 pm and d_2(Si–Si) = 273 pm.[18–20] The latter case is given as being somewhat more stable and corresponds to a singlet diradical, whereby the corresponding intramolecular interaction has significant π character. Because of the energetic proximity of the neighboring minima on the potential hypersurface, this system has been described as an example for bond stretching isomerism.[20, 21]

All E–E distances in the monomers in α-Ba_3Ge_4 and Ba_3Si_4 are approximately equal and correspond to single bonds (d(Si–Si) = 242 pm, $\bar{d}$(Ge–Ge) ≈ 259 pm). Longer bonds are found to occur in both modifications of Ba_3Ge_4, however. In the β form the central bond in the monomer (d(Ge–Ge) = 271.2(7) pm) and in the α form the linking bond in the polymer (d(Ge–Ge) = 287.4(2) pm). The latter is admittedly considerably longer than a single bond, but only slightly different from the long bond in the α form. It is also known from other studies on the somewhat shorter Si–Si single bonds that elongations in the distances of up to 280 pm can occur.[22] If the same should be true of the Ge–Ge bonds described here, as was calculated for the Si–Si bonds in the butterfly molecule, then these long bonds would lie in the expected range.

We determined the electronic structures using the extended Hückel (EH)[23] and the LMTO methods,[24] and calculated the electron localization function ELF.[25] The results are shown in Figures 2 and 3. Both methods lead to very similar densities of states with a small (EH, Figure 2a) or almost nonexistent band gap (LMTO, Figure 2b). This is in agreement with the experimental determination by the van der Pauw method (Figure 2c), although we are unable to distinguish between intrinsic and extrinsic conduction behavior. Comparison of the overlap populations (COOP[26]) for the monomers in the α and β phases as well as for the polymer shows that the bonds in question have a strong, a weak, and a very weak Ge(4s) contribution, respectively (Figures 2e–g).

  1433-7851/98/3723-3315 $ 17.50+.50/0

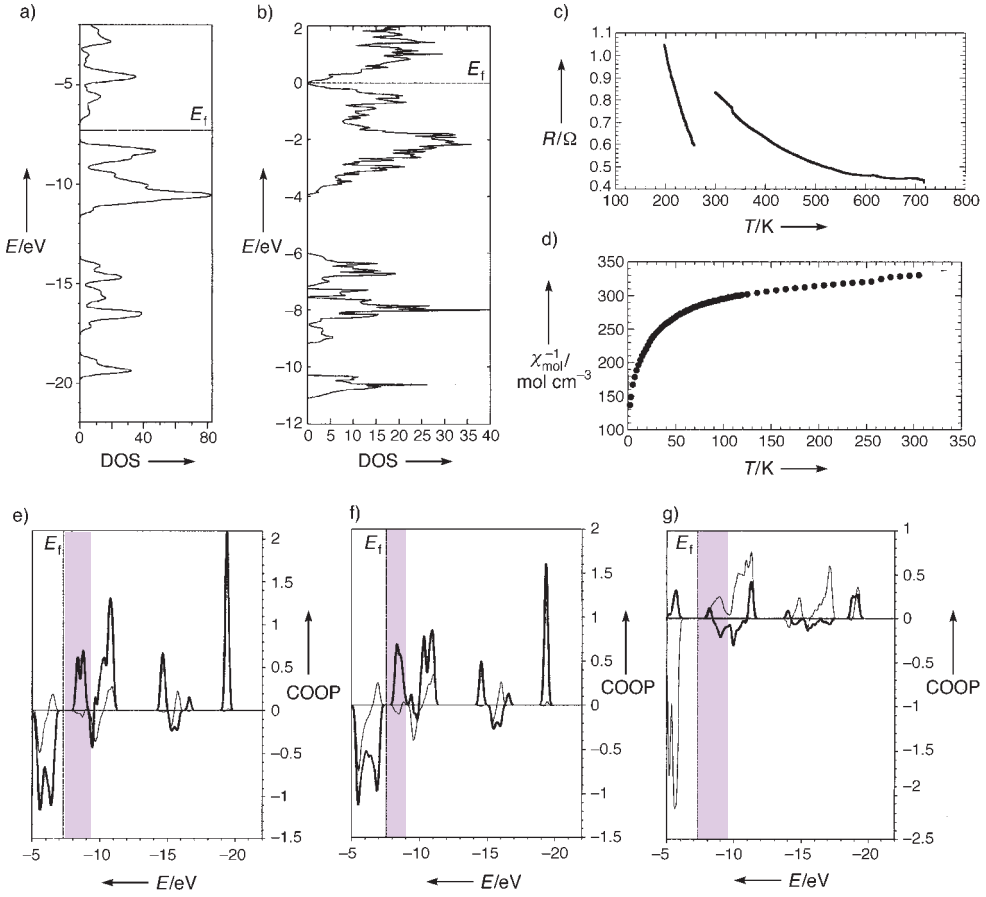

Figure 2. Electronic structure and physical properties of Ba_3Ge_4: a, b) calculated densities of states (DOS); EH (a) and LMTO (b). The DOSs are very similar; as expected, the DOS obtained by the EH calculation has a somewhat larger band gap. c) Temperature dependence of the electrical conductivity according to the four point van der Pauw method; the "band gap" is calculated to about 0.08 eV. The two curves correspond to measurements for two different samples. d) Temperature dependence of the magnetic susceptibility; there is no simple Curie–Weiss dependence. e–g) Overlap populations (COOP) of the intramolecular (thick lines) and intermolecular bonds (thin lines), calculated by the EH method: e) For the isolated anions in α-Ba_3Ge_4 with the relatively short intramolecular Ge–Ge bond (the strong Ge(4s) orbital contribution (population at about −20 eV) is typical for normal σ bonds, the intermolecular interaction is nonbonding). f) For the isolated anions in β-Ba_3Ge_4 with the relatively long intramolecular Ge–Ge bond (here too, the Ge(4s) orbital contribution is in the normal range for σ bonds (population at about −20 eV), the intermolecular interaction is also nonbonding). g) For the polymeric anions in α-Ba_3Ge_4 with the relatively long intermolecular Ge–Ge bond (the Ge(4s) orbital contribution is astonishingly low for σ bonds (population at about −19 eV), in this case the intramolecular interaction is unequivocally nonbonding). The states in the shaded regions were used to calculate the PDEN in Figure 3.

Isosurfaces of the electron localization function (ELF = 0.8) for the monomeric Ge_4^{6-} ions in α- and β-Ba_3Ge_4 are shown in Figures 3a and 3b with one short and one long intramolecular bond, respectively. The extended regions of the free electron pairs on the (2b)Ge atoms are conspicuous; their horse-shoe distributions almost give the impression of a linear part. We know from comparative studies of such highly charged anions that a clear tendency towards sp^2 hybridization occurs, the result of which is a p-type and an sp-type free electron pair. Situations like this have not been considered in the Nyholm–Gillespie rules as yet, and could lead to an extension of the VSEPR theory.[27] This is particularly apparent in the partial electron density (PDEN), which is calculated from the states highlighted in Figure 2e–g close to the Fermi level and shown in Figures 3d–f. The ELF sections through the intermolecular bond in the polymer indicate a weak interaction which results in a double maximum for the EH calculations (Figure 3c). The ELF values from the LMTO calculation are considerably weaker and less extended, partly because the cores can be reproduced better; only one maximum is indicated in this case (Figure 3h). At any rate, it is an interaction which, because of its distance and the strong p-orbital contribution, raises the supposition that a singlet diradical is present. If the ELF is calculated by the LMTO method with an artificially extended Ge–Ge bond of 300 pm, this method also leads to a double maximum on the line connecting the nuclei (Figure 3i). The spatial distribution of these two maxima can be clearly seen in the PDEN in Figure 3f.

We then carried out calculations on a LMTO basis under the assumption of spin polarization, in which in addition to the singlet diradical other radical situations were produced. Surprizingly, all calculations for 0 K converged to a diamagnetic ground state. As the magnetic measurements resulted in a distinct temperature-dependent paramagnetism (Figure 2d), the question still remains as to whether triplet states can occur at higher temperatures, or whether paramagnetic impurities (defects, Nb metal from the wall of the synthesis ampoule) are present. We conclude at any rate that the double maxima in the long bonds indicate an unusual form of the chemical bond and a transition to the diradical form.

Received: July 3, 1998 [Z12089IE]
German version: *Angew. Chem.* **1998**, *110*, 3451–3454

Keywords: electronic structure · electron localization function · solid-state chemistry · Zintl anions

[1] E. Zintl, *Angew. Chem.* **1939**, *52*, 1; E. Zintl, J. Goubeau, W. Dullenkopf, *Z. Phys. Chem. A* **1931**, *154*, 1; *Z. Phys. Chem. B* **1932**, *16*, 183; W. Klemm, *Proc. Chem. Soc. London* **1958**, 329; H. G. von Schnering, *Angew. Chem.* **1981**, *93*, 44; *Angew. Chem. Int. Ed. Engl.* **1981**, *20*, 33; R. Nesper, *Prog. Solid State Chem.* **1990**, *20*, 1.

  1433-7851/98/3723-3316 $ 17.50+.50/0

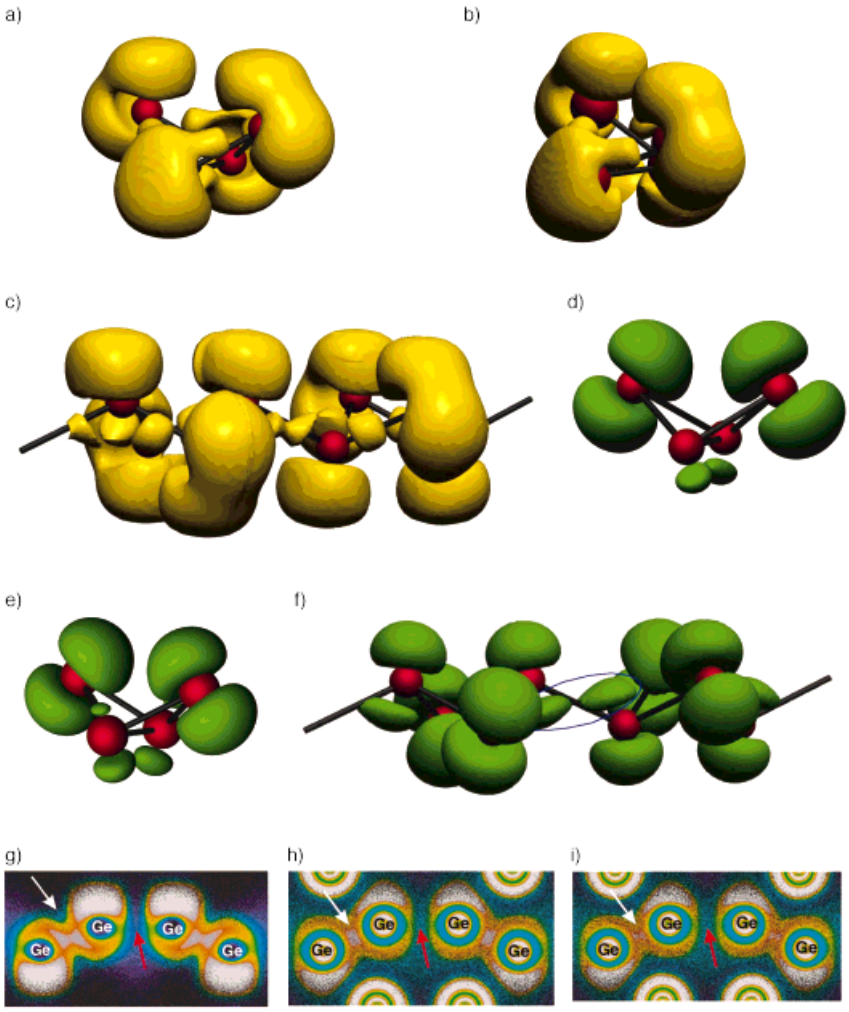

Figure 3. Depiction of the electron localization function ELF for Ba_3Ge_4: three-dimensional ELF isosurfaces (EH; ELF = 0.8): a) For the isolated Ge_4^{6-} in α-Ba_3Ge_4; the spatial requirement of the free electron pairs, with distinct p orbital character on the two-valent Ge atoms, is conspicuous. The central bond can be described as a bridge between the free electron pairs of the three-valent Ge atom. b) For the isolated Ge_4^{6-} in β-Ba_3Ge_4; the general ELF distribution is similar, but the long intramolecular bond is divided into two wedge-shaped pieces, which are attached to the free electron pairs of the three-valent Ge atoms. c) For the polymeric Ge_4^{6-} in α-Ba_3Ge_4; the general ELF distribution is again similar, but instead of the long intramolecular bond, a localization with two maxima between the three-valent Ge atoms occurs. d–f) The corresponding partial densities (PDEN[28]) for states near to the Fermi level for the structural parts in (a–c) show increasing p orbital contributions from (d) to (f) on the (3b) Ge atoms. g–i) Comparison of the ELF from EH and LMTO calculations in two-dimensional sections through the intramolecular (red arrow) and intermolecular bond (white arrow) in the polymer chain of β-Ba_3Ge_4. In all cases, no bonding localization occurs in the corresponding intramolecular region. Whereas the EH calculation (g) for the intermolecular bond clearly leads to two bright localization regions, for the LMTO calculation there is still no separation visible at 278 pm (h). At the extended distance of 300 pm this clearly does occur, however (i).

[2] H. G. von Schnering, *Rheinisch-Westfälische Akademie der Wissenschaften*, lecture N325, p. 7, Westdeutscher Verlag, Opladen **1984**; J. D. Corbett, *Struct. Bonding* **1997**, *87*, 157; H. G. von Schnering, W. Hönle, *Chem. Rev.* **1988**, *88*, 243; B. W. Eichhorn, R. C. Haushalter, *J. Chem. Soc. Chem. Commun.* **1990**, 937; T. F. Fässler, M. Hunziker, *Z. Anorg. Allg. Chem.* **1996**, *622*, 837.

[3] M. Schwarz, Dissertation, Universität Stuttgart, **1987**.

[4] B. Eisenmann, K. H. Janzon, H. Schäfer, A. Weiss, *Z. Naturforsch. B* **1969**, *24*, 457.

[5] A. Currao, J. Curda, R. Nesper, *Z. Anorg. Allg. Chem.* **1996**, *622*, 85.

[6] R. Nesper, A. Currao, S. Wengert in Organosilicon Chemistry II, From Molecules to Materials (Eds.: N. Auner, J. Weis), VCH, Weinheim, **1995**.

[7] S. Wengert, Dissertation no. 12070, ETH Zürich, **1996**.

[8] S. Wengert, A. Currao, R. Nesper, *Chem. Eur. J.* **1998**, *4*, 2244.

[9] N. Wiberg, C. M. Finger, K. Polborn, *Angew. Chem.* **1993**, *105*, 1140; *Angew. Chem. Int. Ed. Engl.* **1993**, *32*, 1054.

[10] T. B. Massalski, *Binary Alloy Phase Diagrams*, 2nd ed., ASM International, **1992**.

[11] K. Turban, H. Schäfer, *Z. Naturforsch. B* **1973**, *28*, 220.

[12] W. Rieger, E. Parthé, *Acta Crystallogr.* **1967**, *22*, 919.

[13] A. Betz, H. Schäfer, A. Weiss, R. Wulf, *Z. Naturforsch. B* **1968**, *23*, 878.

[14] J. Evers, Dissertation, Universität München, **1974**.

[15] Single-phase X-ray samples of α-Ba_3Ge_4 were prepared in a two-stage synthesis. A stoichiometric mixture of the pure elements were initially heated under inert gas in a sealed Nb ampoule for 24 h at 1120 K. The product obtained was finely ground under inert gas, heated for a further 24 h at 1360 K, and then cooled at a rate of 100–500 K h^{-1}. Metastable β-Ba_3Ge_4 at room temperature was not observed at this cooling rate. The compound was obtained in the form of gray, platelike, brittle crystals with a metallic sheen. They are extraordinarily sensitive to air and moisture and decompose in air within a few seconds to give an orange-red powder (presumably GeO). A biting smell was noted.

[16] F. Zürcher, Dissertation, no. 12546, ETH Zürich, **1998**.

[17] α-Ba_3Ge_4 crystallizes with a new structural type (*Cmmm*, $a = 1179.9(6)$, $b = 1221.0(6)$, $c = 1209.7(6)$ pm, $Z = 8$, $R(1083\,F^2(F^2 \geq \sigma(F^2))$, 46 parameters) = 0.031, $R_w(1083\,F^2(F^2 \geq \sigma(F^2))$, 46 parameters) = 0.067, β-Ba_3Ge_4 is stable above 350 °C with Ba_3Si_4 structure ($P4_2/mnm$, $a = 862.1(6)$, $b = 1203.1(8)$ pm, $Z = 4$, $R(310\,F^2(F^2 \geq \sigma(F^2))$, 24 parameters) = 0.054, $R_w(310\,F^2(F^2 \geq \sigma(F^2))$, 24 parameters) = 0.134. Further details on the crystal structure investigation may be obtained from the Fachinformationszentrum Karlsruhe, D-76344 Eggenstein-Leopoldshafen, Germany (fax: (+49) 7247-808-666; e-mail: crysdata@fiz-karlsruhe.de), on quoting the depository numbers CSD-391060 (α-Ba_3Ge_4) and CSD-391061 (β-Ba_3Ge_4).

[18] T. Dabisch, W. W. Schoeller, *J. Chem. Soc. Chem. Commun.* **1986**, 896; W. W. Schoeller, T. Dabisch, T. Busch, *Inorg. Chem.* **1987**, *26*, 4383.

[19] S. Collins, R. Dutler, A. Rauk, *J. Am. Chem. Soc.* **1987**, *109*, 2564.

[20] P. von R. Schleyer, A. F. Sax, J. Kalcher, R. J. Janoschek, *Angew. Chem.* **1987**, *99*, 374; *Angew. Chem. Int. Ed. Engl.* **1987**, *26*, 364.

[21] W.-D. Stohrer, R. Hoffmann, *J. Am. Chem. Soc.* **1972**, *94*, 779.

[22] H. Bock, T. Hauck, C. Näther, N. Rösch, M. Staufer, O. D. Häberlen, *Angew. Chem.* **1995**, *107*, 1439; *Angew. Chem. Int. Ed. Engl.* **1995**, *34*, 1353.

[23] The program EHMACC is based on a computer program by Hoffmann and Lipscomb: R. Hoffmann, W.N. Lipscomb, *J. Chem. Phys.* **1962**, *36*, 2179; M.-H. Whangbo, R. Hoffmann, R.B. Woodward, *Proc. R. Soc. London A* **1979**, *366*, 23; the extended Hückel calculation was carried out without prior charge iterations with the following atomic parameters on the basis of the structural data: Ba: $H_{ii}(6s) = -4.287$ eV, $\varsigma(6s) = 1.236$; $H_{ii}(6p) = -3.036$ eV, $\varsigma(6p) = 1.071$; Ge: $H_{ii}(4s) = -16.0$ eV, $\varsigma(4s) = 2.16$; $H_{ii}(3p) = -9.0$ eV, $\varsigma(3p) = 1.85$.

  1433-7851/98/3723-3317 $ 17.50+.50/0

[24] Program TB-LMTO: M. van Schilfgaarde, T. A. Paxton, O. Jepsen, O. K. Andersen, Max-Planck-Institut für Festkörperforschung, Stuttgart, Germany, Version 4.6, **1994**.
[25] A. D. Becke, K. E. Edgecombe, *J. Chem. Phys.* **1990**, *992*, 5397; A. Savin, R. Nesper, S. Wengert, T. F. Fässler, *Angew. Chem.* **1997**, *109*, 1892; *Angew. Chem. Int. Ed. Engl.* **1997**, *36*, 1808.
[26] R. Hoffmann, *Solids and Surfaces, A Chemists View of Bonding in Extended Structures*, VCH, New York, **1988**.
[27] R. J. Gillespie, *Molecular Geometry*, Van Nostrand Reinhold, London, **1972**.
[28] T. F. Fässler, U. Häussermann, R. Nesper, *Chem. Eur. J.* **1995**, *1*, 625.

The Hydrogen-Bonded Framework of the First Anti-Zeotype: $[\{(H_2NEt_2)_2\}_2(CuCl_4)][AlCl_4]$**

James D. Martin* and Brian R. Leafblad

Zeolites are the archetypal class of porous framework materials whose host–guest interactions have been tailored to a variety of industrial processes such as catalysis and gas separation.[1] Zeolites are constructed from silicate and aluminate building blocks in which the tetrahedral cations are covalently linked by two-coordinate anions (oxygen) into a plethora of micro- and mesoporous frameworks.[2–4] In these systems the size and shape of the pore structure is controlled during synthesis by molecular or cationic templating species. By use of charge-matching techniques, numerous oxide-based framework materials analogous to zeolites have been reported, including frameworks rich in transition metals such as the recently reported cobalt phosphates.[5] We recently demonstrated an extension of such charge-matching techniques to include substitution of framework anions, as well as cations, in the preparation of halozeotypes $[Cu_nZn_{m-n}Cl_{2m}]^{n-}$, which are direct analogues of aluminosilicates.[6] The preparation of other non-oxide zeotype materials has recently been reviewed.[4] Here we describe the first example of an "inverse" charge-matching strategy, by which an anti-zeotype framework structure is constructed from the linkage of tetrahedral anions by two-coordinate cations.

The synthesis of open-framework materials based on principles of structural anti-types, in which the positions of the framework anions and cations are reversed (such as in fluorite, CaF_2, and anti-fluorite structures, Li_2O) has to our knowledge never been reported. Unlike classic zeotype frameworks, in which an anionic or neutral framework is templated by extra-framework cations or molecules, our anti-zeotype constructions, in which tetrahedral anions are linked by two-coordinate cations, can be utilized to prepare cationic frameworks templated by noncoordinating extra-framework anions. Such anion templating is expected to yield both novel open-framework structures and unique properties.[7]

Previously, several metal-organic cationic frameworks have been prepared in which neutral, bidentate ligands link cationic metal centers into covalent networks.[4, 8, 9] However, in these metal-organic frameworks, the cationic metal centers are coordinatively saturated by the two-coordinate linker ligands such that the internal surface of the framework cavity which surrounds the anionic template consists of the neutral ligands. By contrast, in our anti-zeotype constructions, the internal surface of the open-framework voids will be composed of two-coordinate cationic linking units. This cationic surface of the framework void may be exploitable to increase anion-binding affinities.

Because of the utility of hydrogen bonding for the construction of supramolecular assemblies, dialkylammonium cations were examined as potential two-coordinate cations to link $[MCl_4]^{n-}$ tetrahedral anions. In spite of the importance of hydrogen bonding between cations and anions for supramolecular assembly and molecular recognition in biological systems, to date only a small number of organic and metal-organic supramolecular hydrogen-bonded frameworks have been constructed using exclusively ionic components,[7, 10–12] compared with the number of hydrogen-bonded assemblies prepared using neutral molecules as donors and acceptors.[13–16] Nevertheless the strength of interionic hydrogen bonds of around 40–190 kJ mol^{-1}[10] make such ionic constructions attractive for the preparation of more robust framework structures. In this present work, we exploit the hydrogen-bonding ability of dialkylammonium cations to link $[CuCl_4]^{3-}$ tetrahedral anions into the novel anti-zeotype framework $[\{(H_2NEt_2)_2\}_2(CuCl_4)]^+$, in which $[AlCl_4]^-$ anions fill the framework void. This cationic partial structure is shown in Figure 1. Such hydrogen-bonded frameworks are not expected to provide the rigid structures found for covalent zeolite-type frameworks; however, Yaghi et. al. have recently demonstrated microporosity in a framework constructed from hydrogen-bonded metal-organic complexes.[15]

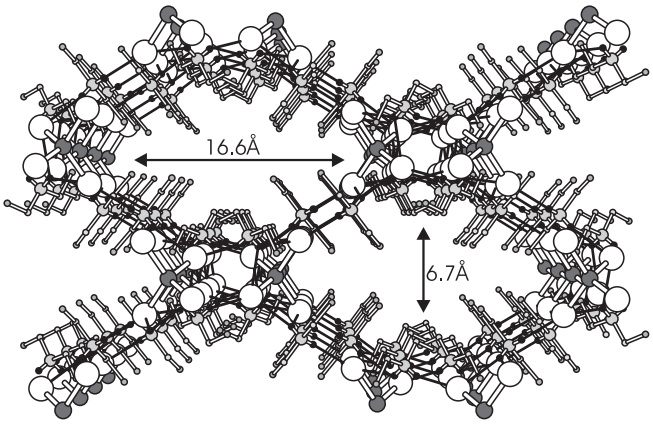

Figure 1. Cationic partial structure of **1**. The hydrogen-bonding contacts are indicated by solid lines. Cl: large open spheres, Cu: large black spheres, N: large gray spheres, C: small gray spheres, H: small black spheres.

[*] Prof. J. D. Martin, B. R. Leafblad
Department of Chemistry
North Carolina State University
Raleigh, NC 27695-8204 (USA)
Fax: (+1) 919-515-5079
E-mail: jdmartin@ncsu.edu

[**] This work was supported by the National Science Foundation, a CAREER award (DMR-9501370), and an instrumentation grant (CHE-9509532). J.D.M. is a Cottrell Scholar of the Research Corporation.

  1433-7851/98/3723-3318 $ 17.50+.50/0